Journal of Applied Polymer Science

Poly(styrene-maleic anhydride) functionalized graphene oxide

Longfei Zhou,[1,2] Haihui Liu,[1,2] Xingxiang Zhang[1,2]
[1]Key Laboratory of Advanced Textile Composite Materials of Ministry of Education, Tianjin 300387, China
[2]School of Material Science and Engineering, Tianjin Polytechnic University, Tianjin 300387, China
Correspondence to: X. Zhang (E-mail: zhangpolyu@aliyun.com)

ABSTRACT: In this study, poly(styrene–maleic anhydride) functionalized graphene oxide (SMAFG) was fabricated with *in situ* polymerization. The sample was characterized with Raman spectroscopy, Fourier transform infrared spectroscopy, thermogravimetric analysis, transmission electron microscopy, and ultraviolet–visible absorption. The results of the experiments show that the thermal stability of SMAFG was improved significantly, and it also possessed a good dispersion in *N*,*N*-dimethylformamide, *N*,*N*-dimethylacetamide, aniline, and certain organic solvents. The calculated Hildebrand parameter of SMAFG was 23.8 $MPa^{1/2}$. This new method will broaden the applications of graphene, and the experiment showed that it could effectively improve the strength of polyamide 6 (PA6) compared with the pure PA6 fiber. The tensile strength of the SMAFG/PA6 composite fiber improved 29%, and the Young's modulus improved 33%, so this kind of functionalized graphene oxide can be used in the preparation of polymeric composites. © 2015 Wiley Periodicals, Inc. J. Appl. Polym. Sci. **2015**, *132*, 41987.

KEYWORDS: composites; fibers; grafting; graphene and fullerenes; nanotubes

Received 20 August 2014; accepted 14 January 2015
DOI: 10.1002/app.41987

INTRODUCTION

Graphene is a new kind of carbon material, which consists of a single layer of sp^2 hybridized carbons, and a hexagonal network structure. As a result of its special two-dimensional structure, it possesses excellent mechanical, thermal, and electrical properties. According to previous reports,[1–10] graphene possesses a tensile strength of approximately 125 GPa, whereas its Young's modulus is approximately to 1.1 TPa. In addition, an individual graphene sheet has a large surface area, which is close to 2600 m^2/g. This surface area serves to improve its combinations with the polymer matrix.[2,3,11] The key issue in the application of graphene is its dispersion and functionalization. The methods used to obtain functionalized graphene include covalent and noncovalent functionalization.[2,12,13] Strom *et al.*[14] grafted phenylalanine to graphene through the use of nitrene addition. Lee *et al.*[15] reported 4-aminobenzoic acid grafted carbon nanotubes by Friedel–Crafts acylation, and Liu *et al.*[16] obtained functionalized graphene with the same method. However, functionalized graphene obtained by these methods only provides a small number of reactive groups.

In this study, a simple method was used to graft poly(styrene–maleic anhydride) (SMA) to graphene oxide (GO). Because of the presence of acid anhydride groups, the functionalized GO formed covalent bonds with many kinds of polymer chains. The synthesis of the functionalized graphene is given in Figure 1. Because of the presence of SMA chains, the compatibility of graphene with some polymer matrixes will be improved [e.g., polyamide 6 (PA6)], so it could be used in the preparation of polymeric composites.

EXPERIMENTAL

Materials

Graphite powder (8000 mesh) was obtained from Qingdao Henglide Graphite Co., Ltd. Styrene, maleic anhydride and azobisisobutyronitrile (AIBN) were purchased from Tianjin Guangfu Reagents Co. The Raman spectrum was recorded with a DXR Raman microscope (Thermo Scientific) with a laser wavelength of 532 nm. The Fourier transform infrared (FTIR) spectrum was recorded on a Bruker Vector 22 spectrometer. The micrographs of graphene were observed with transmission electron microscopy (TEM; Hitachi H-800), with the instrument was operating at an accelerating voltage of 100 kV. Thermogravimetric analysis (TGA) plots were obtained with thermogravimetry (Netzsch STA 409 PC/PGTG–DTA) in the range of room temperature to 800°C under an inert air atmosphere with a heating rate of 10°C/min. The ultraviolet absorbance plots were obtained with an ultraviolet–visible spectrophotometer (TU-180, wavelength = 270 nm). The mechanical properties of the fibers were obtained with a fiber tensile tester (LLY-06), the fiber length was 10 mm, and the rate was 10 mm/min.

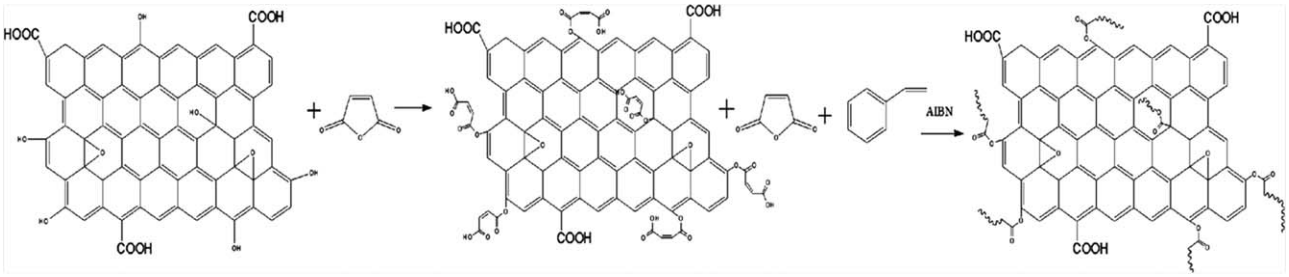

Figure 1. Synthesis of SMAFG by *in situ* polymerization (∿∿∿ = SMA chains).

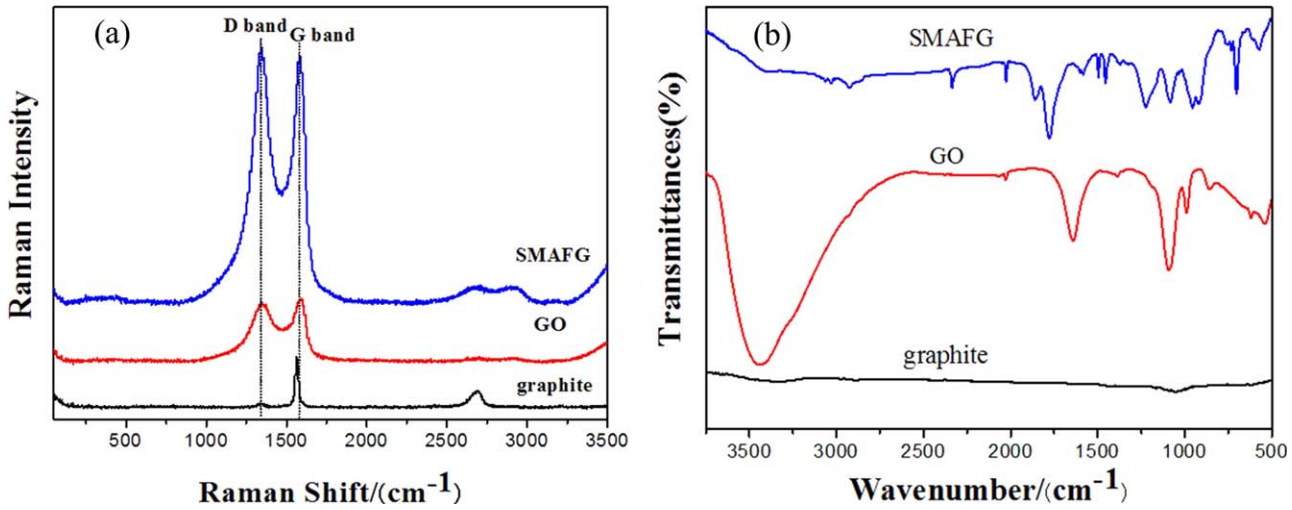

Figure 2. Raman and FTIR spectra of graphite, GO, and SMAFG. [Color figure can be viewed in the online issue, which is available at wileyonlinelibrary.com.]

Sample Preparation

GO was synthesized from natural graphite with the modified Hummers' method.[17] GO (0.5 g) was mixed with toluene solution, which was dissolved in excess maleic anhydride. After 10 min of ultrasonication, the mixture was poured into a 500-mL, three-necked flask with an N_2 inlet. The mixture reacted at room temperature and was continuously stirred for 8 h. After this, 8.0 g of styrene, 8.3 g of maleic anhydride, and 0.4 g of AIBN were then added. The reaction was kept at 80°C for 6 h. Finally, the black solid was washed with acetone three times and vacuum-dried at 80°C for 24 h.

RESULTS AND DISCUSSION

In Figure 2(a), the intense band at about 1340 cm^{-1} (D band) corresponded to the number of sp^3 carbons and reflected the structural defects of the graphite sheet. The band at about 1580 cm^{-1} (G band) was a characteristic peak of the sp^2 carbons.[18] The intensities of the D bands of GO and poly(styrene–maleic anhydride) functionalized graphene oxide (SMAFG) were significantly higher than those of graphite. This was attributed to the covalent binding of graphene with oxygenous groups and SMA molecular chains. The groups and molecular chains caused a large number of defects to be formed on the graphene sheets.

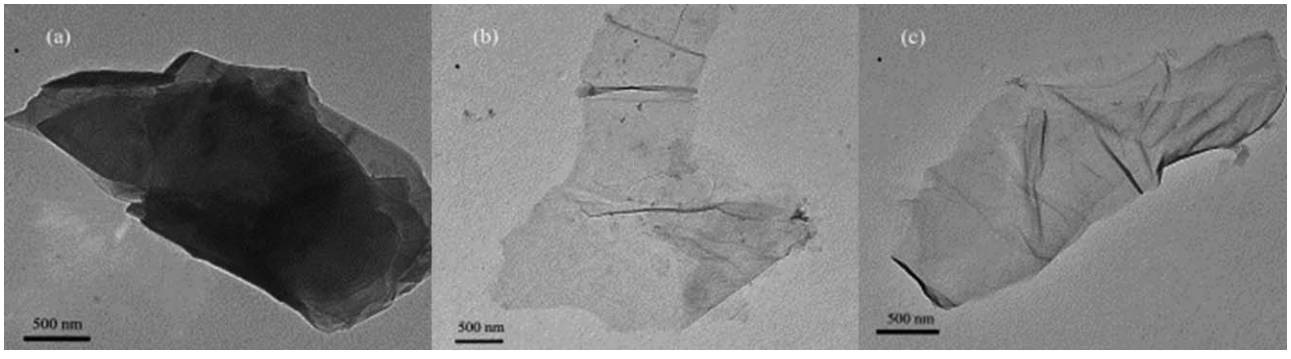

Figure 3. TEM micrographs of the samples: (a) graphite, (b) GO, and (c) SMAFG.

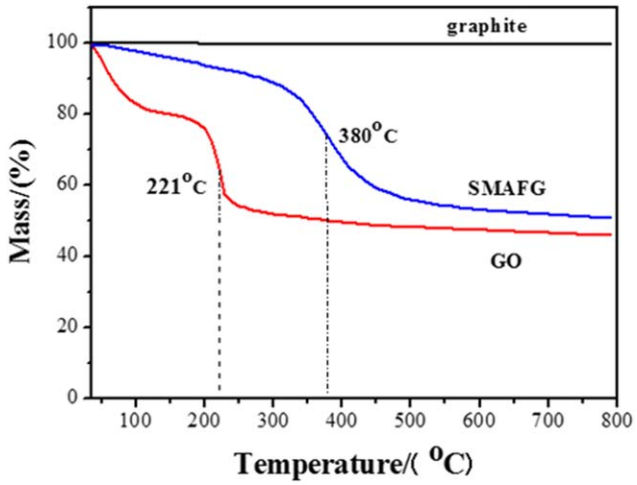

Figure 4. TGA plots of graphite, GO, and SMAFG. [Color figure can be viewed in the online issue, which is available at wileyonlinelibrary.com.]

The intensity ratio of D band and G band (I_D/I_G) ratio could be used as an indication of the extent of the functionalization reaction and disorder. The I_D/I_G ratio increased from 0.16 to 0.95 and 1.02 after the oxidation reaction and modification by SMA, respectively. This indicated that the extent of disorder increased because of the presence of oxygenous groups and polymer chains.

Figure 2(b) shows the FTIR spectra of graphite, GO, and SMAFG. The peaks at 1857 and 1779 cm^{-1} of SMAFG were assigned to the C═O stretching bands of maleic anhydride. The peaks at 1596, 1497, and 1454 cm^{-1} were assigned to the skeleton vibration of the benzene ring.[19] The peak at 706 cm^{-1} was assigned to the C—H bending vibrations of styrene. In addition, the peak at 1221 cm^{-1} was the characteristic peak of the C—O stretching vibrations. These results indicate that SMA was grafted on graphene.

As shown in Figure 3, compared with the multilayer structure of graphite, the number of layers of GO and SMAFG was visibly reduced. Some folds appeared on the surface. This was due to the presence of certain oxygenous groups or molecular chains on the surface. These folds were conductive to the thermal stability of graphene and provided space limitations on a nanoscale. This enhanced the binding between graphene and the polymer matrix, and it could restrict the movement of the polymer chains. It, thereby, increased the strength and Young's modulus.

Figure 4 shows the TGA plots of graphite, GO, and SMAFG. The mass loss of GO below 110°C was assigned to the release of water, and the main mass loss between 208 and 248°C was due to the decomposition of oxygenous groups. Compared with GO, no distinguishable weight loss was observed below 220°C for SMAFG, and the main weight loss occurred at 380°C, which was roughly 160°C higher than that of GO. This was due to the removal of the SMA chains that were grafted on the surface of the GO sheets.[9] The results indicate that the thermal stability of SMAFG was improved significantly.

The Hildebrand parameter (δ) was introduced to investigate the dispersion of graphene in polymers. According to Hansen's theory, the cohesive energy density comprises the dispersion (d), polarity (p), and hydrogen-bonding portion (H). δ is the total cohesion energy, and it can be seen as the sum of these three components.[20]

Usually, δ_i (where $i = d$, p, or H) was used to represent the three components, as shown in eq. (1):

$$\delta^2 = \delta_d^2 + \delta_p^2 + \delta_H^2 \quad (1)$$

The three Hansen parameters are then given as follows:

$$\delta_i = \sum_{\text{solvent}} C\delta_{i,\text{sol}} \Big/ \sum_{\text{solvent}} C \quad (2)$$

where C is the dispersability in a given solvent and $\delta_{i,\text{sol}}$ is the ith Hansen parameter in a given solvent.[20,21]

According to Lambert–Beer law ($A = \alpha CL$, where A is the absorbance, α is the absorption coefficient, C is the concentration of graphene, and L is the thickness of liquid layer), eq. (2) can be simplified as follows:

$$\delta_i = \sum_{\text{solvent}} A\delta_{i,\text{sol}} \Big/ \sum_{\text{solvent}} A \quad (3)$$

Ten solvents were chosen as the dispersants of SMAFG. As shown in Figure 5(a), SMAFG possesses a good dispersion in N-methyl pyrrolidone (NMP), *N,N*-dimethylacetamide (DMAc), and certain organic solvents, and the solubility parameters of various solvents are shown in Table I. Figure 5(e) shows that the dispersion of SMAFG associated with the hydrogen-bonding cohesion parameter (δ_H), and the range of δ_H are shown by the dotted lines in Figure 5(e) within 7.2–13.7 $MPa^{1/2}$. Six kinds of dispersants capable of preferably dispersing graphene were then selected to calculate δ of SMAFG. The values of δ_d, δ_p, and δ_H obtained with eq. (3) were 18.1, 11.4, and 10.5 $MPa^{1/2}$, respectively. Then, the value of δ calculated by eq. (1) was 23.8 $MPa^{1/2}$. The same method was used to calculate δ_d, δ_p, and δ_H of GO. The absorbance–δ_i plots of the GO dispersions are shown in Figure 6, and the solubility parameters of the various solvents are shown in Table II. The values of δ_d, δ_p, and δ_H obtained with eq. (3) were 16.8, 11.9, and 16.3 $MPa^{1/2}$, respectively. Then, the value of δ calculated by eq. (1) was 26.3 $MPa^{1/2}$. The Hansen parameters of PA6 ($\delta_d = 18.9$ $MPa^{1/2}$, $\delta_p = 7.9$ $MPa^{1/2}$, and $\delta_H = 11.7$ $MPa^{1/2}$) were obtained from the literature,[22] and the value of δ calculated by eq. (1) was 23.6 $MPa^{1/2}$. The results indicate that δ of SMAFG was closer to that of PA6; this inferred that the dispersability of SMAFG was improved in the PA6 matrix by the principle of like dissolves like.[22]

SMAFG reacted with 6-aminocaproic acid and ε-caprolactam at 180°C for 2 h under stirring (excluded the air by N_2). Then, the temperature was raised to 275°C and kept for 2 h.[12] Finally, the powders were washed with acetone five times, and then, the PA6-grafted SMAFG (SMAFG–PA6) was obtained. As shown in Figure 7, compared with SMAFG, no peaks occurred at 1857 and

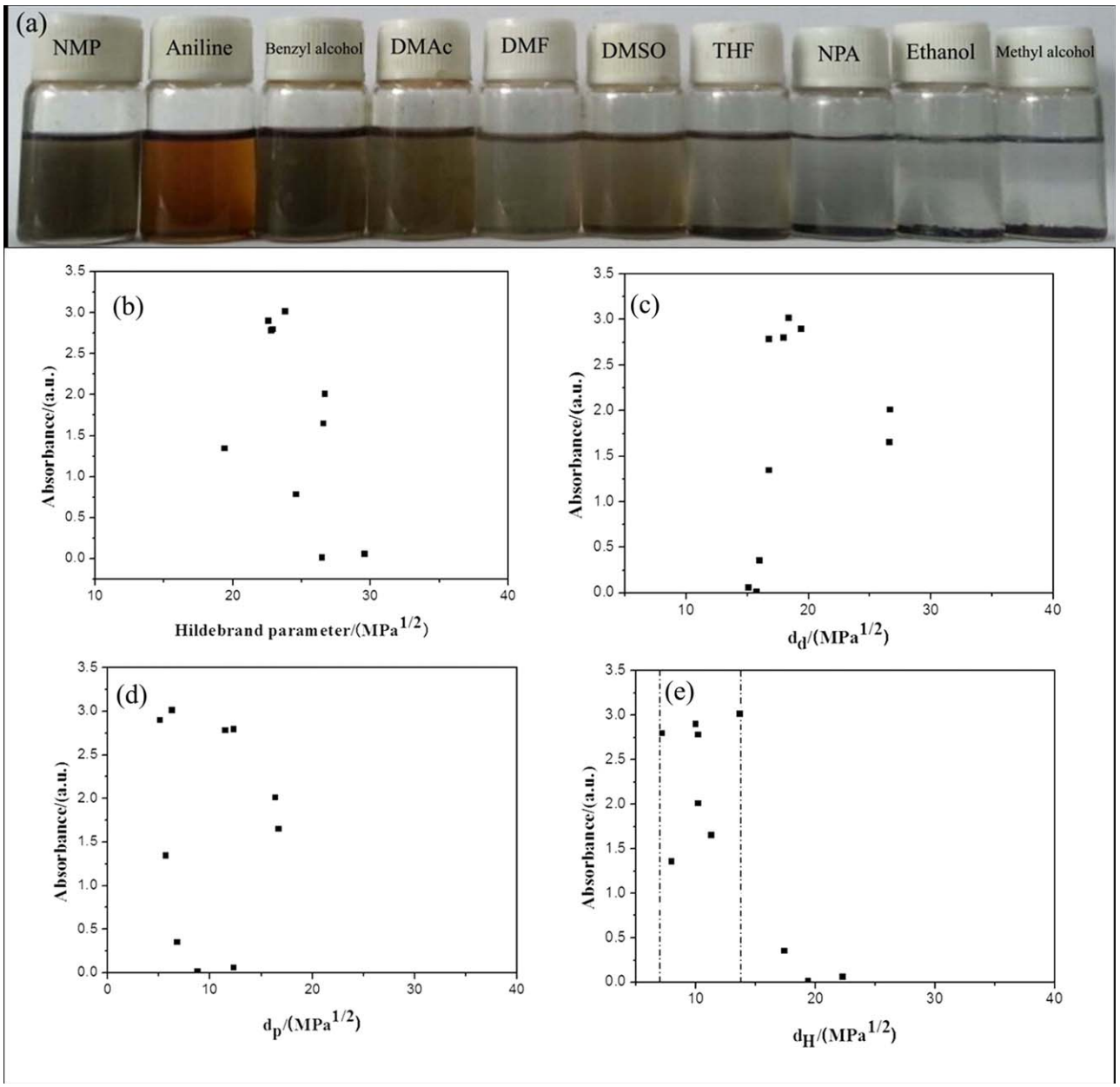

Figure 5. (a) SMAFG dispersed in different solvents and (b) absorbance–δ, (c) absorbance–δ_d, (d) absorbance–δ_p, and (e) absorbance–δ_H plots of the SMAFG dispersions. DMF = *N*,*N*-dimethylformamide; DMSO = dimethyl sulfoxide; THF = tetrahydrofuran; NPA = 1-propyl alcohol; d_d = contribution from dispersion forces; d_p = contribution from polar interactions; d_H = contribution factor from hydrogen bonding. [Color figure can be viewed in the online issue, which is available at wileyonlinelibrary.com.]

Table I. Solubility Parameters of the Various Solvents of SMAFG

Name	Molecular formula	δ_d (MPa$^{1/2}$)	δ_p (MPa$^{1/2}$)	δ_H (MPa$^{1/2}$)	δ (MPa$^{1/2}$)
DMF	$HCON(CH_3)_2$	17.4	16.7	11.3	26.6
DMSO	$(CH_3)_2—S—O$	18.4	16.4	10.2	26.7
DMAc	$CH_3CON(CH_3)_2$	16.8	11.5	10.2	22.8
THF	C_4H_8O	16.8	5.7	8.0	19.4
N-Methyl pyrrolidone	C_5H_9NO	18.0	12.3	7.2	22.9
Aniline	C_6H_7N	19.4	5.1	10.2	22.6
Benzyl alcohol	C_7H_8O	18.4	6.3	13.7	23.8
Ethanol	C_2H_5OH	15.8	8.8	19.4	26.5
1-Propyl alcohol	C_3H_8O	16.0	6.8	17.4	24.6
Methyl alcohol	CH_3OH	15.1	12.3	22.3	29.6

DMF, *N*,*N*-dimethylformamide; DMSO, dimethyl sulfoxide; THF, tetrahydrofuran.

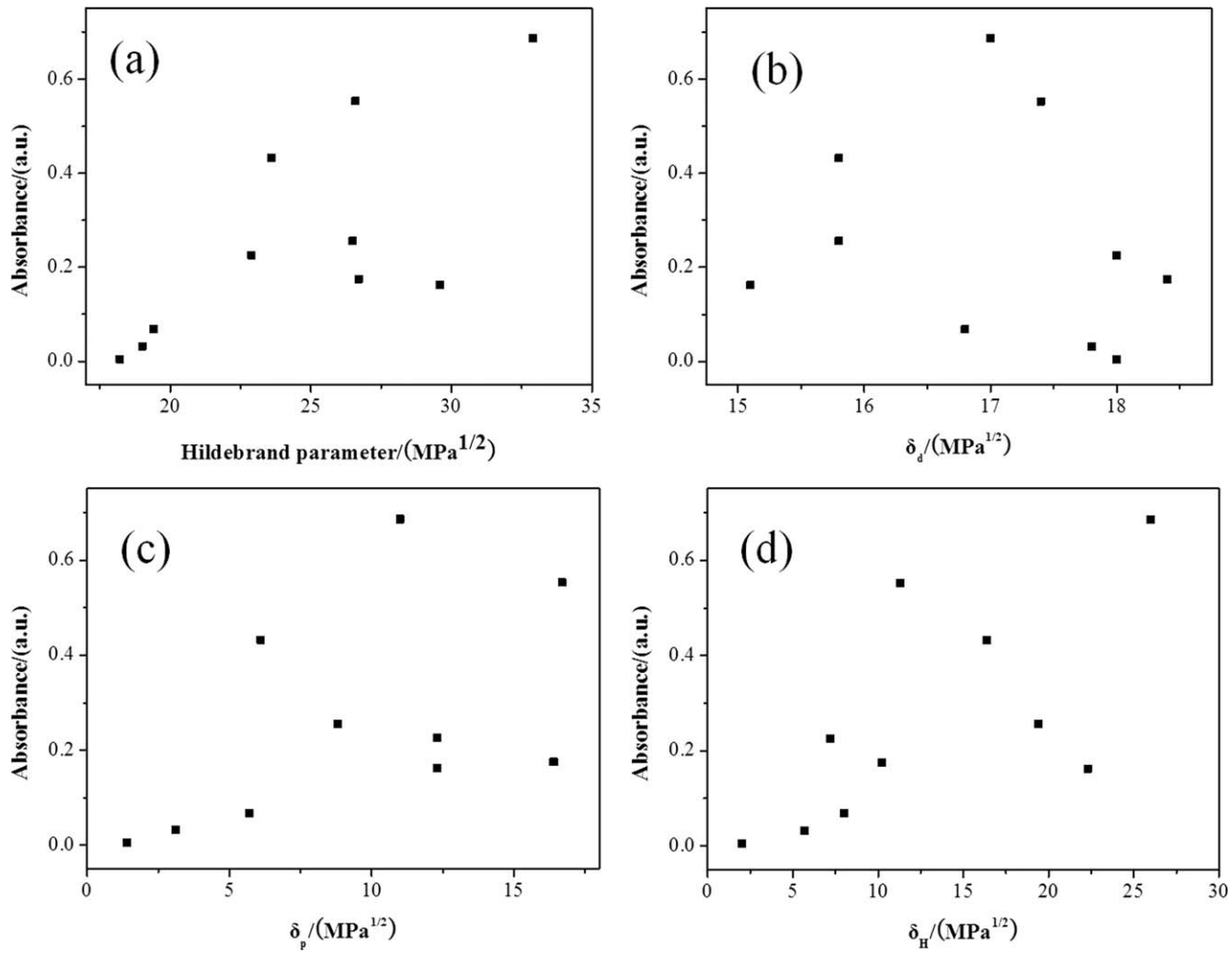

Figure 6. (a) Absorbance–δ, (b) absorbance–δ_d, (c) absorbance–δ_p, and (d) absorbance–δ_H plots of the GO dispersions.

1779 cm^{-1}. This indicated that the groups of maleic anhydride reacted with 6-aminocaproic acid and ε-caprolactam. The new peak at 3169 cm^{-1} was assigned to N—H stretching bands of amide, and that at 1664 cm^{-1} was assigned to the N—H bending vibration of amide. The peak at 1406 cm^{-1} was the characteristic peak of the C—N stretching bands of amide. These characteristic peaks indicated that SMAFG formed covalent bonds with PA6. In addition, the digital photograph showed that SMAFG–PA6 dispersed evenly in formic acid, so SMAFG had a good dispersion in the PA6 matrix.

Table II. Solubility Parameters of the Various Solvents of GO

Name	Molecular formula	δ_d ($MPa^{1/2}$)	δ_p ($MPa^{1/2}$)	δ_H ($MPa^{1/2}$)	δ ($MPa^{1/2}$)
DMF	$HCON(CH_3)_2$	17.4	16.7	11.3	26.6
Ethylene glycol	$(HOCH_2)_2$	17	11	26	32.9
N-Methyl pyrrolidone	C_5H_9NO	18.0	12.3	7.2	22.9
THF	C_4H_8O	16.8	5.7	8.0	19.4
Isopropyl alcohol	C_3H_8O	15.8	6.1	16.4	23.6
Toluene	C_7H_8	18.0	1.4	2.0	18.2
Chloroform	$CHCl_3$	17.8	3.1	5.7	19.0
Ethanol	C_2H_5OH	15.8	8.8	19.4	26.5
DMSO	$(CH_3)_2$—S—O	18.4	16.4	10.2	26.7
Methyl alcohol	CH_3OH	15.1	12.3	22.3	29.6

DMF, *N*,*N*-dimethylformamide; DMSO, dimethyl sulfoxide; THF, tetrahydrofuran.

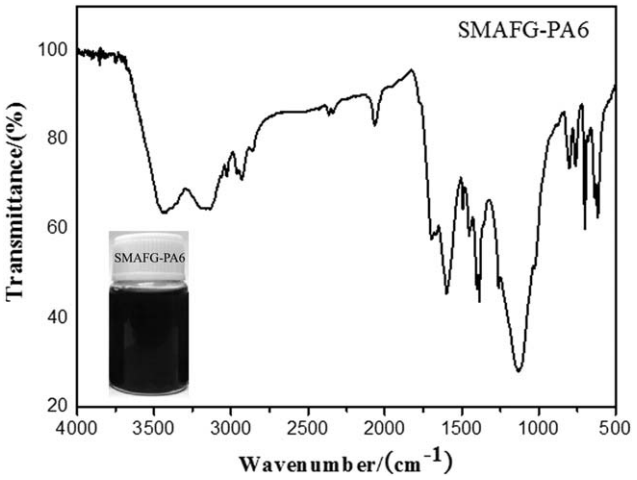

Figure 7. FTIR spectra of SMAFG–PA6 and digital photograph of SMAFG–PA6 dispersed in formic acid.

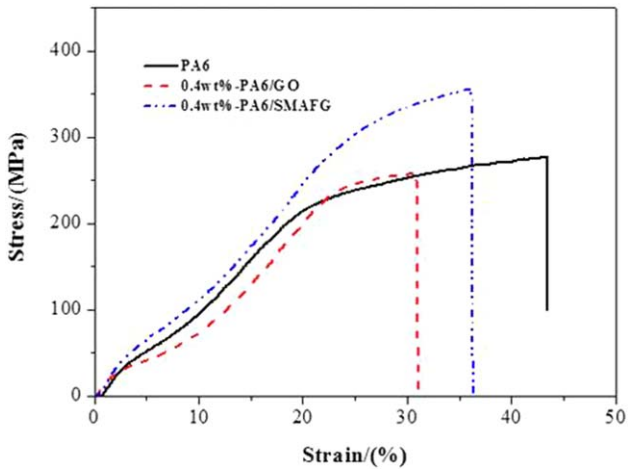

Figure 9. Stress–strain curves of the pure PA6 fiber and 0.4 wt % PA6/GO and 0.4 wt % PA6/SMAFG composite fibers. [Color figure can be viewed in the online issue, which is available at wileyonlinelibrary.com.]

To study the application of SMAFG in the polymer matrix, the pure PA6 fiber and SMAFG/PA6 composite fiber were spun, and their mechanical properties were tested. As shown in Figure 8, SMAFG was uniformly dispersed in PA6 and formed a cladding layer of PA6 surrounding SMAFG, and the graphene was not pulled out from the matrix. This indicated that strong chemical bonds were formed between SMAFG and PA6. This indicated that the stress on the matrix was transferred to the graphene effectively, and this restricted the movement of the polymer chains of PA6. Thereby, the mixture of SMAFG effectively improved the mechanical properties of the composite fibers, and this was proven by Figure 9.[23]

Figure 9 shows the stress–strain curves of the pure PA6 fiber, PA6/GO composite fibers with a 0.4 wt % GO loading, and PA6/SMAFG composite fibers with a 0.4 wt % SMAFG loading. It was obvious that the addition of SMAFG into PA6 had a significant influence on the mechanical properties of the PA6 matrix. The tensile strength of pure PA6 was 277 MPa, and the Young's modulus was 1.32 GPa. In contrast, the tensile strength of the PA6/GO composite fiber was 258 MPa, and the Young's modulus was 1.42 GPa. This showed has less effective enhancement on the mechanical properties of the composite fiber. We assumed that the existence of van der Waal's forces between GO sheets and shear forces during the process of preparation caused the aggregation of GO sheets, so the GO could not be uniformly dispersed in the PA6 matrix. The presence of aggregates caused stress concentration in the composite fiber and resulted in a decrease in the strength of the fiber. However, the tensile strength of the PA6/SMAFG composite fiber was 356 MPa, and the Young's modulus was 1.75 GPa. Compared with the pure PA6 fiber, the tensile strength of the fiber was improved by 29%, and the Young's modulus was improved by 33%. This was due to the good dispersion of SMAFG and the covalent bonds between the acid anhydride groups and amino groups of the PA6 matrix. These were the two most important factors in the improvement of the mechanical properties.

CONCLUSIONS

SMA was effectively grafted on the surface of the graphene with *in situ* polymerization. Compared with GO, the thermal stability of SMAFG was significantly improved, and this was due to the formation of chemical bonds between the SMA molecular chains.

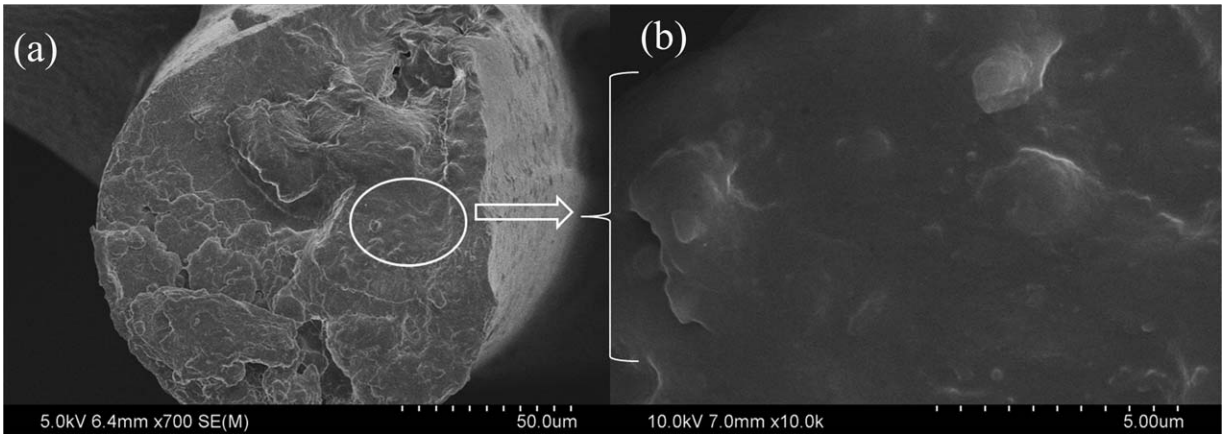

Figure 8. SEM micrographs of the fracture surface of the SMAFG–PA6 composite fiber containing 0.4 wt % SMAFG.

GO was more stable than the oxygen-containing groups on the surface of GO. The calculated solubility parameter of SMAFG was 23.8 $MPa^{1/2}$. The reactive groups and high strength of graphene made it suitable for use in the preparation of polymeric composites, such as PA6. The results show that SMAFG had a good dispersion in PA6, and it formed covalent bonds with the matrix, so it could improve the mechanical properties of polymer materials. These properties will also make graphene suitable for wide applications in the field of material fabrication.

ACKNOWLEDGMENTS

This study was funded by the Key Project in Application of Basic and Frontier Project of Tianjin Municipal (contract grant number grant 13JCZDJC32100).

REFERENCES

1. Geim, A. K.; Novoselov, K. S. *Nat. Mater.* **2007**, *6*, 183.
2. Kuila, T.; Bose, S.; Mishra, A. K.; Khanra, P.; Kim, N. H.; Lee, J. H. *Prog. Mater. Sci.* **2012**, *57*, 1061.
3. Lee, C.; Wei, X.; Kysar, J. W.; Hone, J. *Science* **2008**, *321*, 385.
4. Li, H.; Liang, S.; Pan, Y.; Li, G.; He, L.; Li, J. *Funct. Mater. Lett.* **2014**, *7*, 1.
5. You, F.; Wang, D.; Li, X.; Liu, M.; Dang, Z. M.; Hu, G. H. *J. Appl. Polym. Sci.* **2014**, *131*, 1.
6. Kim, H.; Abdala, A. A.; Macosko, C. W. *Macromolecules* **2010**, *43*, 6515.
7. Zhao, J.; Wang, X.; Zhou, W.; Zhi, E.; Zhang, W.; Ji, J. *J. Appl. Polym. Sci.* **2013**, *130*, 3212.
8. Du, X.; Skachko, I.; Barker, A.; Andrei, E. Y. *Nat. Nanotechnol.* **2008**, *3*, 491.
9. Geim, A. K. *Science* **2009**, *324*, 1530.
10. Li, X. S.; Zhu, Y. W.; Cai, W. W.; Borysiak, M.; Han, B.; Chen, D.; Piner, R. D.; Colombo, L.; Ruoff, R. S. *Nano Lett.* **2009**, *9*, 4359.
11. Ramanathan, T.; Abdala, A. A.; Stankovich, S.; Dikin, D. A.; Herrera-Alonso, M.; Piner, R. D.; Adamson, D. H.; Schniepp, H. C.; Chen, X.; Ruoff, R. S.; Nguyen, S. T.; Aksay, I. A.; Prud'homme, R. K.; Brinson, L. C. *Nat. Nanotechnol.* **2008**, *3*, 327.
12. Fang, M.; Wang, K.; Lu, H.; Yang, Y.; Nutt, S. *J. Mater. Chem.* **2009**, *19*, 7098.
13. Chatterjee, S.; Nüesch, F. A.; Chu, B. T. T. *Chem. Phys. Lett.* **2013**, *557*, 92.
14. Strom, T. A.; Dillon, E. P.; Hamilton, C. E.; Barron, A. R. *Chem. Commun.* **2010**, *46*, 4097.
15. Lee, H. J.; Han, S. W.; Kwon, Y. D.; Tan, L. S.; Baek, J. B. *Carbon* **2008**, *46*, 1850.
16. Liu, H.; Hou, L.; Peng, W.; Zhang, Q.; Zhang, X. *J. Mater. Sci.* **2012**, *47*, 8052.
17. Xu, Z.; Gao, C. *Macromolecules* **2010**, *43*, 6716.
18. Ferrari, A. C.; Meyer, J. C.; Scardaci, V.; Casiraghi, C.; Lazzeri, M.; Mauri, F.; Piscanec, S.; Jiang, D.; Novoselov, K. S.; Roth, S.; Geim, A. K. *Phys. Rev. Lett.* **2006**, *97*, 187401.
19. Yan, D.; Yang, G. *Mater. Lett.* **2009**, *63*, 298.
20. Bergin, S. D.; Sun, Z.; Rickard, D.; Streich, P. V.; Hamilton, J. P.; Coleman, J. N. *ACS Nano* **2009**, *3*, 2340.
21. Hernandez, Y.; Lotya, M.; Rickard, D.; Bergin, S. D.; Coleman, J. N. *Langmuir* **2010**, *26*, 3208.
22. Hansen, C. M. Hansen Solubility Parameters—A User's Handbook; CRC: Boca Raton, FL, **2007**; Chapter 4.
23. Liu, H. H.; Peng, W. W.; Hou, L. L.; Wang, X. C.; Zhang, X. X. *Compos. Sci. Technol.* **2013**, *81*, 61.